GaN-based MSM photovoltaic ultraviolet detector structure modeling and its simulation*

Chen Yiren(陈一仁)†, Song Hang(宋航), Li Dabing(黎大兵), Sun Xiaojuan(孙晓娟), Li Zhiming(李志明), Jiang Hong(蒋红), and Miao Guoqing(缪国庆)

Key Laboratory of Excited State Processes, Changchun Institute of Optics, Fine Mechanics and Physics, Chinese Academy of Sciences, Changchun 130033, China

Abstract: Based on the principles of metal–semiconductor–metal Schottky barrier photodetectors (MSM-PD), using the carrier rate equations, the circuit simulation model of a GaN-based MSM photovoltaic ultraviolet detector is constructed through an appropriately equivalent process. By using the Pspice analytical function of Cadence soft on the model, the relationship between the photocurrent and the terminal voltage under different UV light powers is analyzed. The result shows that under the given UV power, the photocurrent increases and tends to become saturated gradually as the terminal voltage of the device increases, and that under different UV powers, the photocurrent increases with increasing incident power. Then the analysis of the relationship between the photocurrent and the terminal voltage under the different ratios of interdigital electrode space and width is carried out when the UV power is given. The results show that when the ratio of interdigital electrode space and width (L/W) equals 1, the photocurrent tends to be at a maximum.

Key words: MSM structure; simulation; equivalent circuit; ultraviolet detector
DOI: 10.1088/1674-4926/32/3/034005 **PACC:** 2940P; 7280E; 7340S

1. Introduction

A GaN ultraviolet detector (UVPD) has broad application prospects in the fields of optical communication, optical interconnection, optical detection, optical information processing and so on, due to its advantages of fast response, high sensitivity, simple structure, low cost and easy integration of planar device structure. In addition, the GaN-based metal–semiconductor–metal (MSM) structure ultraviolet detector with its high breakdown voltage, low noise, strong ability to adapt to the environment and anti-radiation, and working without a filter has become a hot topic of GaN ultraviolet detector research.

With the rapid development of integrated circuit computer-aided design (CAD), it becomes an important part in the design of optoelectronic integrated circuits through the establishment of a reasonable simulation model for photoelectric detectors and then simulating and researching their properties by computer. In this way, for the development of a new device, one can optimize the process of a device, shorten the development cycle, reduce the cost and so on. Currently, the equivalent circuit model of MSM structure photodetectors usually uses the one presented by Sano[1]. This consists of a conductance and a capacitor in parallel, that is,

$$I_{\rm op} = G(t)V_{\rm g} + C(t)\frac{{\rm d}V_{\rm g}}{{\rm d}t}, \tag{1}$$

where $I_{\rm op}$ is the terminal current of the photoelectric detector and $V_{\rm g}$ is the terminal voltage,

$$G(t) = \frac{C_{\rm m}qNv_{\rm n}(C_{\rm f}F_{\rm g}) + C_{\rm m}qv_{\rm p}C_{\rm f}F_{\rm g}}{V_{\rm g}L_{\rm g}} + G_{\rm dark}, \tag{2}$$

$$C(t) = C_{\rm T} + C_{\rm p}, \tag{3}$$

where $G_{\rm dark}$ is the dark conductivity; $C_{\rm p}$ is the parasitic capacitance; $C_{\rm m}$ is the introduced parameter for the model; $C_{\rm f}$ is a parameter introduced for considering the attenuation of the electric field in the absorption region; $C_{\rm T}$ is for the storage capacitor produced by electric charge when lighting condition; $v_{\rm n}(v_{\rm p})$ represents the electron (hole) drift velocity; and $L_{\rm g}$ is the width between the two electrodes.

The shortcoming of the model is to ignore the non-linear relationship between the dark current and terminal voltage of the photoelectric detector, instead replacing with a dark conductance, which would be a very good approximation when the impact of dark current characteristic to the device isn't accurately considered, but larger error. In this paper, Sano's model of an MSM structure photodetector will be consulted, and a GaN-based MSM photovoltaic ultraviolet detector simulation model will be proposed that consists of the current source, capacitor and voltage-controlled current source, and then simulating and analyzing based on the model.

2. MSM structure model

The structure of a GaN-based photovoltaic MSM-UVPD is composed of two back-to-back Schottky diodes, which use

* Project supported by the National Natural Science Foundation of China (Nos. 60976011, 51072196, 51072195) and the National Basic Research Program of China (No. 2011CB301901).
† Corresponding author. Email: yiren_chen@126.com
Received 26 August 2010, revised manuscript received 20 October 2010

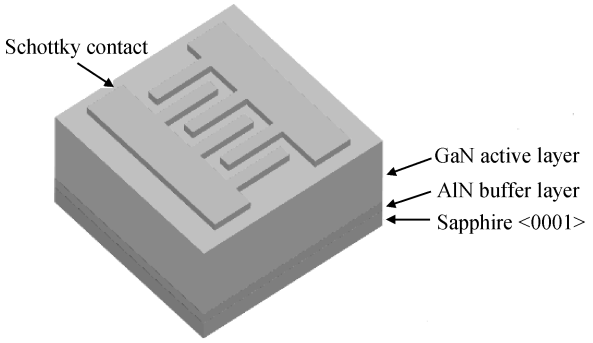

Fig. 1. Structure of GaN-based MSM UV detector.

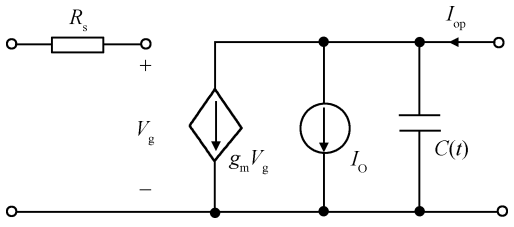

Fig. 2. Equivalent circuit of the GaN-based MSM UV detector.

the photovoltaic effect of a semiconductor to achieve UV detection. Its basic principle is that ultraviolet light irradiates the detector, pairs of electron and a hole are separated under the effect of built-in electric field and generate photoproduction voltage accordingly. When the output circuit loops, the photocurrent is produced[2]. Figure 1 shows the structure of a GaN-based MSM UV detector. This consists of several components: a (0001) plane sapphire substrate; an AlN buffer layer, typically several tens of nanometers, which is used to hold up the substrate's defects extended to the absorption layer; a GaN absorption layer (active layer), generally a micron order of magnitude, which plays a decisive role in the performance of the device; and Ni/Au interdigital electrode. If the thickness of the absorption layer increases, the light absorption is increased and the reception sensitivity is improved, but because of the increasing depth, the electric field is weakened. Accordingly, the carriers' drift velocity decreases and the responsive bandwidth is reduced[3].

Based on the model presented by Sano, an improved model (composed of the current source, a capacitor and a voltage-controlled current source) is proposed in this paper.

$$I_{\rm op} = I_{\rm o} + g_{\rm m} V_{\rm g} + C(t)\frac{{\rm d}V_{\rm g}}{{\rm d}t}, \tag{4}$$

where $I_{\rm op}$ stands for the terminal current of the ultraviolet detector and $V_{\rm g}$ is the terminal voltage of the detector.

In Eq. (4), the first item $I_{\rm o}$ is the excess carriers in the absorption region contributing to the terminal current of the MSM-UVPD; the second item $g_{\rm m}V_{\rm g}$ stands for the voltage-controlled current source in which $g_{\rm m}$ (transconductance) describes the control role of the terminal voltage of the detector to dark current $I_{\rm dark}$ without UV irradiation; the third item is the current generated by capacitance $C(t)$ (including the depletion layer capacitance $C_{\rm p}$ without UV irradiation and the storage capacitance $C_{\rm T}$ caused by the charge generated under UV irradiation) under the action of the terminal voltage applied to the detector. Therefore, we get the equivalent circuit of the GaN-based MSM UV detector (show in Fig. 2). As can be seen from the model, to study the terminal current of the detector, we just need to consider the excess carriers in the absorption region, the dark current and the intrinsic capacitance contributing to the current when induced terminal voltage, respectively, and then all of the current coming to the stack is the analytic equation of the terminal current.

Firstly, based on the rate equations of excess carriers in the absorption region, the contribution of the excess carriers to the terminal current is studied. The rate equations[4, 5] of the excess carriers (electron and hole) in the absorption region of the MSM photodetector are as follows,

$$\begin{cases} \dfrac{{\rm d}N}{{\rm d}t} = G - \dfrac{N}{\tau_{\rm nt}} - \dfrac{N}{\tau_{\rm nr}}, \\ \dfrac{{\rm d}P}{{\rm d}t} = G - \dfrac{P}{\tau_{\rm pt}} - \dfrac{P}{\tau_{\rm pr}}. \end{cases} \tag{5}$$

In Eq. (5), N (P) stands for the quantity of excess electrons (holes) in the absorption region; $\tau_{\rm nt}$ ($\tau_{\rm pt}$) is the electron (hole) drift transit-time; $\tau_{\rm nr}$ ($\tau_{\rm pr}$) is the electron (hole) recombining lifetime; and G is the number of photo-generated carriers in absorption region per unit time.

$$G = \frac{P_{\rm in}(1-r)\dfrac{L}{L+W}\left(1-{\rm e}^{-\alpha d}\right)}{h\nu}, \tag{6}$$

$$\tau_{\rm nt} = \frac{L}{v_{\rm n}},\ \tau_{\rm pt} = \frac{L}{v_{\rm p}}. \tag{7}$$

In Eqs. (6) and (7), r stands for the reflection coefficient of the device surface; α stands for the absorption coefficient per unit length of the device's absorption layer corresponding to the wavelength of light; $P_{\rm in}$ is the incident optical power to the device; L is the spacing of the Ni/Au interdigital electrode; W is the width of the interdigital electrode; d stands for the thickness of the absorption layer (active layer); and $h\nu$ is the photon energy

Under the fixed electric field, the correcting formula of the carrier velocity is[1]

$$\begin{cases} v_{\rm n} = \dfrac{\mu_{\rm n}F_{\rm g} + v_{\rm ns}\left(F_{\rm g}/F_{\rm th}\right)^4}{1+\left(F_{\rm g}/F_{\rm th}\right)^4}, \\ v_{\rm p} = \dfrac{\mu_{\rm p}F_{\rm g}}{1+\mu_{\rm p}F_{\rm g}/v_{\rm ps}}. \end{cases} \tag{8}$$

In Eq. (8), $\mu_{\rm n}$ ($\mu_{\rm p}$) is the electron (hole) mobility; $v_{\rm ns}$ ($v_{\rm ps}$) is the electron (hole) saturation drift velocity; $F_{\rm g}$ stands for the average electric field ($= V_{\rm g}/L$) between the interdigital electrodes; and $F_{\rm th}$ is the threshold electric field. Substituting Eqs. (6)–(8) into Eq. (5), we have

$$N = \frac{P_{\text{in}}\tau_{\text{nr}}L(1-r)\dfrac{L}{L+W}\left(1-\mathrm{e}^{-\alpha d}\right)\left[V_{\text{g}}^4+\left(F_{\text{th}}L\right)^4\right]}{h\nu\left[\tau_{\text{nr}}\left(\mu_{\text{n}}V_{\text{g}}L^3F_{\text{th}}^4+\upsilon_{\text{ns}}V_{\text{g}}^4\right)+L\left(L^4F_{\text{th}}^4+V_{\text{g}}^4\right)\right]}\times\left(1-\exp\left\{-\frac{\tau_{\text{nr}}\left[\mu_{\text{n}}V_{\text{g}}L^3F_{\text{th}}^4+\left(\upsilon_{\text{ns}}V_{\text{g}}\right)^4\right]+L\left(V_{\text{g}}^4+F_{\text{th}}^4L^4\right)}{\tau_{\text{nr}}L\left(V_{\text{g}}^4+F_{\text{th}}^4L^4\right)}t\right\}\right), \tag{9}$$

$$P = \frac{P_{\text{in}}\tau_{\text{pr}}L(1-r)\dfrac{L}{L+W}\left(1-\mathrm{e}^{-\alpha d}\right)\left(L\upsilon_{\text{ps}}+\mu_{\text{p}}V_{\text{g}}\right)}{h\nu[\tau_{\text{pr}}\mu_{\text{p}}\upsilon_{\text{ps}}V_{\text{g}}+L(L\upsilon_{\text{ps}}+\mu_{\text{p}}V_{\text{g}})]}\times\left\{1-\exp\left[-\frac{\tau_{\text{pr}}\mu_{\text{p}}\upsilon_{\text{ps}}V_{\text{g}}+L(L\upsilon_{\text{ps}}+\mu_{\text{p}}V_{\text{g}})}{\tau_{\text{pr}}L(L\upsilon_{\text{ps}}+\mu_{\text{p}}V_{\text{g}})}t\right]\right\}. \tag{10}$$

Substituting Eqs. (9) and (10) into $I_{\text{o}} = I_{\text{n}} + I_{\text{p}} = \dfrac{C_{\text{m}}qNv_{\text{n}}\left(C_{\text{f}}F_{\text{g}}\right)+C_{\text{m}}qPv_{\text{p}}\left(C_{\text{f}}F_{\text{g}}\right)}{L}$ [6], we get I_{o} as follows,

$$\begin{aligned} I_{\text{o}} &= \frac{C_{\text{m}}q(C_{\text{f}}F_{\text{g}})G}{L}\times(Nv_{\text{n}}+Pv_{\text{p}}) \\ &= \frac{C_{\text{m}}q(C_{\text{f}}F_{\text{g}})G}{L}\times\left(\frac{v_{\text{n}}\tau_{\text{nr}}L\left[V_{\text{g}}^4+(F_{\text{th}}L)^4\right]}{\tau_{\text{nr}}\left(\mu_{\text{n}}V_{\text{g}}L^3F_{\text{th}}^4+v_{\text{ns}}V_{\text{g}}^4\right)+L\left(L^4F_{\text{th}}^4+V_{\text{g}}^4\right)}\right. \\ &\quad\times\left\{1-\exp\left\{-\frac{\tau_{\text{nr}}\left[\mu_{\text{n}}V_{\text{g}}L^3F_{\text{th}}^4+(v_{\text{ns}}V_{\text{g}})^4\right]+L\left(V_{\text{g}}^4+F_{\text{th}}^4L^4\right)}{\tau_{\text{nr}}L(V_{\text{g}}^4+F_{\text{th}}^4L^4)}t\right\}\right\} \\ &\quad\left.+\frac{v_{\text{p}}\tau_{\text{pr}}L(L\upsilon_{\text{ps}}+\mu_{\text{p}}V_{\text{g}})}{\tau_{\text{pr}}\mu_{\text{p}}\upsilon_{\text{ps}}V_{\text{g}}+L(L\upsilon_{\text{ps}}+\mu_{\text{p}}V_{\text{g}})}\times\left\{1-\exp\left[-\frac{\tau_{\text{pr}}\mu_{\text{p}}\upsilon_{\text{ps}}V_{\text{g}}+L(L\upsilon_{\text{ps}}+\mu_{\text{p}}V_{\text{g}})}{\tau_{\text{pr}}L(L\upsilon_{\text{ps}}+\mu_{\text{p}}V_{\text{g}})}t\right]\right\}\right). \end{aligned} \tag{11}$$

Secondly, in the absence of UV irradiation, dark current (I_{dark}) will be generated when voltage is applied to the detector, the dark current mainly comes from several transport mechanism, as follows: the Schottky thermionic emission from the interface between the metal and the semiconductor; tunneling current; and electronic transition under strong electric field. In the absence of a UV radiation environment, the transmission mechanisms mentioned above generate dark current only related to the terminal voltage, and therefore we use a voltage-controlled current source to simulate the dark current, ignoring the instance of punch through voltage (V_{RT}), that is,

$$I_{\text{dark}} = g_{\text{m}}V_{\text{g}}, \tag{12}$$

where $g_{\text{m}} = \beta_{\text{D}}\left(\lambda_{\text{D}}+1/V_{\text{g}}\right)\tanh\left(\alpha_{\text{D}}V_{\text{g}}\right)$ stands for the transconductance of voltage-controlled current source, in which β_{D} is the responsivity parameter under dark current; α_{D} is the flat-band voltage parameter; and λ_{D} is the internal current gain coefficient of the detector.

Finally, the capacitance in the model indicates as Eq. (3), parallelly composes by the generated carrier storage effect (C_{T}) when the device is irradiated by ultraviolet light and the parasitic capacitance C_{P}, and the storage capacitance (C_{T}) formed by the carrier produced by the electron and hole, so C_{T} is calculated as

$$\frac{1}{C_{\text{T}}} = \frac{1}{C_{\text{ga}}(t)} + \frac{1}{C_{\text{gc}}(t)}. \tag{13}$$

Then arranged

$$C(t) = C_{\text{T}} + C_{\text{P}} = \frac{C_{\text{ga}}(t)C_{\text{gc}}(t)}{C_{\text{ga}}(t)+C_{\text{gc}}(t)} + C_{\text{P}}. \tag{14}$$

In Eq. (14), $C_{\text{ga}}(t) = C_{\text{c}}A_{\text{a}}\sqrt{\dfrac{qN\left(t-\tau_{\text{d}}\right)\varepsilon_0\varepsilon_{\text{s}}}{S_{\text{e}}dV_{\text{g}}(t)}}$, $C_{\text{gc}}(t) = C_{\text{c}}A_{\text{c}}\sqrt{\dfrac{qP\left(t-\tau_{\text{d}}\right)\varepsilon_0\varepsilon_{\text{s}}}{S_{\text{e}}dV_{\text{g}}(t)}}$.

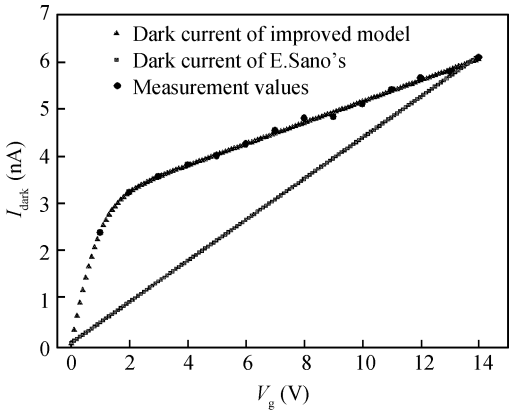

Fig. 3. Simulation result of GaN-based MSM-UVPD's dark current compared with the measurements and Sano's results.

Here, C_{c} is the introducing parameter of the model; A_{a} (A_{c}) is the anode (cathode) area of the interdigital electrode; S_{e} is the effective photic area; τ_{d} is the formation time of the space-charge region under the electrode; ε_0 stands for the vacuum dielectric constant; and ε_{s} is the relative dielectric constant of GaN.

3. MSM model simulation and analysis

Using the model constructed above, the simulation was carried out by the Pspice function of Cadence soft, and the specific parameters used during the process are shown in Table 1. Figure 3 shows the simulation result of the GaN-based MSM-UVPD's dark current characteristics, compared with the measurement result and Sano's simulation curve. It can be seen from the diagram that the model makes up for the shortage of Sano's model, which considers the nonlinear relationship between the photodetector's dark current and terminal voltage,

Table 1. Model parameters of GaN-based MSM-UVPD.

Symbol	Value	Symbol	Value	Symbol	Value
L	3 μm	ε_s	9	T_{nr}	0.2 ns
W	3 μm	λ	360 nm	T_{pr}	0.65 ns
r	0.19	d	2 μm	C_m	10
S_e	6.29×10^{-12} m^2	α	1.0×10^7	C_p	0.1 pF
A_a	6.1×10^{-12} m^2	μ_n	1100 cm^2/(V·s)	R_s	0.001
A_c	6.1×10^{-12} m^2	μ_p	30 cm^2/(V·s)	λ_D	0.077
C_f	0.02	v_{ns}	2.5×10^7 cm/s	β_D	2.89×10^{-9}
C_c	0.5	v_{ps}	2.5×10^7 cm/s	α_D	1.0
C_{no}	$1.0.\times10^{-12}$	F_{th}	4.2×10^8 V/cm		

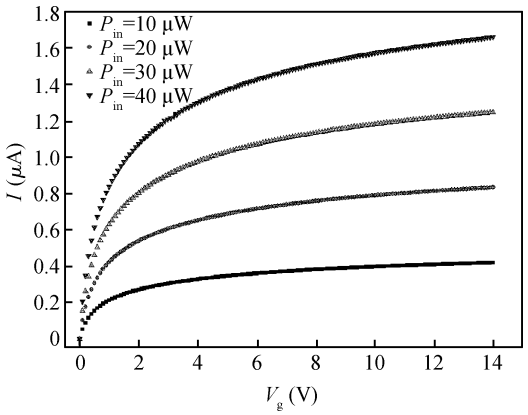

Fig. 4. Relationship between photocurrent and terminal voltage under different UV light powers.

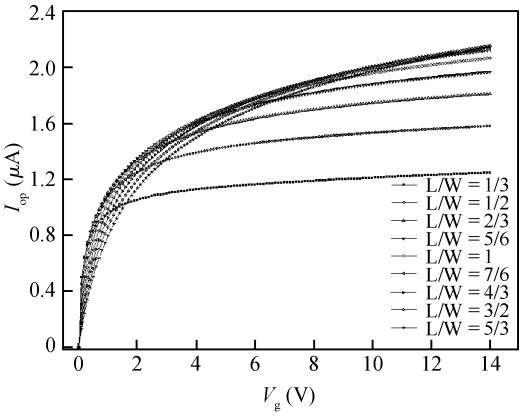

Fig. 5. Relationship between the photocurrent and terminal voltage under different interdigital electrode spaces and width ratios.

so the simulation result is more objective. Figure 4 shows the relationship between the photocurrent and the terminal voltage under different UV light powers when the interdigital width and distance are 3 μm. When the UV power is given, with the increment of the device's terminal voltage, the photocurrent increases and tends to be saturated. This is because the terminal voltage increases, the electric field between the interdigital electrodes gradually increases, which makes the carrier drift rate increase, and then the transit-time shorten, therefore, the carriers' composite probability reduces and the photocurrent increases. But when the electric field reaches a certain level, because the incident light power is constant, the number of carriers generated becomes the maximum and the photocurrent becomes saturated. Under different UV powers, the photocurrent increases with the increment of incident power, and this is related to the energy conversion.

Figure 5 shows the relationship between the photocurrent and the terminal voltage about the different ratios of interdigital electrode width and space under a certain UV power. It can be found from the curve, when the interdigital space and width ratio (L/W) is less than 1, that the photocurrent increases with the increment of the interdigital space (L), and all increase with the increment of terminal voltage and tend to saturation; under the same voltage, the amplitude of the photocurrent's increment diminishes as the interdigital space (L) increases. This is because the interdigital space is smaller than the width, the effective area receiving the incident light is smaller and the quantum efficiency is lower. However, when the interdigital space and width ratio (L/W) is larger than 1, although the effective area receiving the incident light power increases, if the incident light power keeps constant, the number of carriers excited reach a maximum, so the saturated photocurrent remains unchanged. Since $L > W$, when the terminal voltage is lower, the electric field between the interdigital electrodes is weaker than $L < W$, therefore, carrier drift velocity is small and transit-time turn longer, thus combined probability turn larger, as a result, photocurrent is smaller than that of $L < W$ when the terminal voltage is smaller.

4. Conclusion

In summary, an improved model based on Sano's is investigated. In the model, the voltage-controlled current source introduced is equivalent to the dark current of the device, which reasonably considers the nonlinear relationship between the photodetector's dark current and the terminal voltage, making the simulation results more realistic. Through simulation, when the interdigital electrode space and width are given, the relationship between the photocurrent and the terminal voltage under different UV light power is analyzed first. The results indicate that when the UV power is given, the photocurrent increases and tends to become saturated gradually as the terminal voltage of the device increases, and that under different UV power, the photocurrent increases with the increment of incident power. Then the analysis of the relationship between the photocurrent and the terminal voltage under the different ratios of interdigital electrode space and width is carried out when the UV power is given. The result shows that when the

ratio of the interdigital electrode space and the width (L/W) = 1, the photocurrent tends to be a maximum. This study will provide useful reference for the optimization of the photoelectric device's techniques.

References

[1] Sano E. A device model for metal–semiconductor–metal photodetectors and its applications to optoelectronic integrated circuit simulation. IEEE Trans Electron Devices, 1990, 37(9): 1964

[2] Yang Hong. The study of GaN-based photovoltaic MSM structure ultraviolet detector. Master Dissertation, University of Electronic Science and Technology, Chengdu, China, 2009 (in Chinese)

[3] Chen Weiyou, Yang Shuren, Liu Shiyong. Optoelectronic devices circuit model and the circuit-level simulation of OEIC. Beijing: National Defence Industry Press, 2001

[4] Chen Weiyou, Liu Shiyong. The research of metal–semiconductor–metal photodetector circuit model. Chinese Journal of Electronics, 1994, 16(3): 327

[5] Ma Liqin, Lu Qisheng, Du Shaojun, et al. Imitation of the instantaneous change behaviors of photoconductive detectors. Chinese Journal of Lasers, 2004, 31(3): 342

[6] Fan Hui, Lu Yutian. Improved numerical model of metal–semiconductor–metal photodetector. Chinese Journal of Lasers, 2007, 34(8): 1032